Hindawi Publishing Corporation
Journal of Nanomaterials
Volume 2012, Article ID 583417, 8 pages
doi:10.1155/2012/583417

Research Article

Hydrothermal Synthesis of Hydrangea-Like F-Doped Titania Microspheres for the Photocatalytic Degradation of Carbamazepine under UV and Visible Light Irradiation

Miaomiao Ye, Yulong Yang, Yan Zhang, Tuqiao Zhang, and Weiyun Shao

Institute of Municipal Engineering, Zhejiang University, Hangzhou 310058, China

Correspondence should be addressed to Weiyun Shao, shaowy@zju.edu.cn

Received 12 September 2011; Accepted 23 October 2011

Academic Editor: Somchai Thongtem

Hydrangea-like F-doped TiO_2 microspheres have been synthesized on a large scale by a simple hydrothermal process using potassium titanium oxalate as the titanium source, ammonium fluoride and hydrogen peroxide as the etchant. The photocatalytic activities were evaluated using carbamazepine as the target organic molecule under UV and visible light irradiation. Structural characterization indicates that the hydrangea-like TiO_2 microspheres, with an average diameter of 2.80 μm, are composed of numerous anatase TiO_2 petals. Moreover, it is found that both the NH_4F and H_2O_2 dosages have important effects on the formation of the hydrangea-like structures. In addition, photocatalytic experiments show that the hydrangea-like TiO_2 microspheres calcined at 500°C exhibit high photocatalytic efficiency under both UV and visible light irradiation. The enhanced photocatalytic activity can be attributed to the successful fluorine doping, good crystallinity, and the unique nanostructures.

1. Introduction

Heterogeneous photocatalysis using nanosized TiO_2 catalyst under ultraviolet light illumination is an efficient method for the purification of wastewater [1–3]. However, a major barrier to the widespread use of TiO_2 as photocatalyst is its relatively large optical band gap (E_g = 3.2 eV), which limits its photoresponse to visible light [4, 5]. To overcome this limitation, approaches such as mental (or anion) doping, nonmental (or cations) doping, and compositing with other semiconductors have been developed [6, 7]. Among them, it has been found that fluorine doping is the most effective process as it not only can promote the activity of TiO_2 by slowing down the recombination of photogenerated electrons and holes [8–10] but also can induce a visible-light-driven photocatalysis by the creation of oxygen vacancies [11, 12].

On the other hand, in a practical photocatalytic process, it is very difficult to separate and recover these finely powdered TiO_2 from a solution. Recently, three-dimensional (3D) hierarchical structures closely packed with different building bricks have attracted considerable attention not only because of their high surface-to-volume ratios for the improvement of photocatalytic activity but also because of the large size of the complete structures for enhancing of separation efficiency [13, 14]. Therefore, it is still scientific importance to explore novel 3D TiO_2 microspheres with visible light activity and high separation efficiency [15]. In this paper, we report a hydrothermal approach for the synthesis of hydrangea-like F-doped TiO_2 microspheres. The as-prepared products were then characterized by XRD, SEM, TEM, and XPS techniques. The photocatalytic activities of the products before and after calcination at 500°C were evaluated by photocatalytic degradation of carbamazepine under UV and light-emitting diode (LED) light irradiation.

2. Experimental Procedures

Typically, 0.7 g of potassium titanium oxalate was dissolved in 15 mL of distilled water, then 15 mL of 30% H_2O_2, 0.4 mL of 37% HCl, and 400 mg of NH_4F is added to the solution. After five minutes of stirring, the final mixture was directly transferred into a 50 mL Teflon-lined stainless autoclave. The autoclave was maintained at 140°C for 24 h and afterwards allowed to cool to room temperature naturally. Finally, the

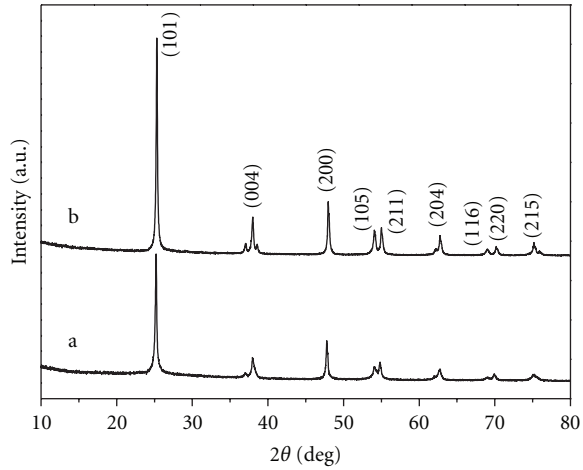

Figure 1: XRD patterns of the as-prepared hydrangea-like F-doped TiO_2 microspheres before and after calcinations at 500°C.

white precipitate was collected, washed with distilled water and ethanol three times, respectively, then dried at 80°C for 12 h, and calcined in air at 500°C for 2 h.

The crystalline structure of the sample was characterized by X-ray diffraction (XRD) with Cu Kα radiation (λ = 1.5406 Å). The size and morphology of the sample were analyzed using a scanning electron microscopy (SEM, Hitachi S-4800) and a transmission electron microscopy (TEM, Phillips Tecnai 10) with an accelerating voltage of 100 kV. The BET surface area and pore size distribution of the product were measured by N_2 adsorption-desorption test (Quantachrome, ASIC-2 measuring instrument). The UV-visible absorption diffuse reflectance spectra were measured on a TU-1901 spectrophotometer equipped with a labsphere diffuse reflectance accessory. The X-ray photoelectron spectroscopy (XPS) measurements were carried out using a VG ESCA Lab Mark II system with Mg Kα excitation.

Photocatalytic degradation of carbamazepine under UV and blue LED light irradiation was carried out in a Pyrex cylindrical batch photoreactor (containing 400 mL reaction slurry, as shown in previous work [2]) and a 100 mL beaker (containing 80 mL reaction slurry, as shown previously [16]), respectively. Agitation was provided by magnetic stirrer. The aqueous slurry, prepared with a given amount of catalyst 1.0 g/L and carbamazepine in concentration of 0.1×10^{-5} mol/L, was stirred in the dark for 30 min to ensure that the carbamazepine was adsorbed to saturation on the catalysts. A 10 W UV lamp (254 nm, GPH212T5L/4, Germany) and a 3 W blue LED lamp (~470 nm, Exploit 220024, China) were used as UV and visible light source, respectively.

The concentration of carbamazepine was determined by HPLC (Agilent 1200, USA) provided with a UV-Vis detector. A 4.6 mm × 250 mm (5 μm) XDB-C18 column was used. The analysis was carried out isocratically with an 60/40 (v/v) methanol/water mobile phase, and the flow rate was set at 1.0 mL/min.

3. Results and Discussion

The XRD patterns of the hydrangea-like F-doped TiO_2 microspheres before and after calcinations at 500°C for 2 h are shown in Figure 1. Before calcination, the strong and sharp diffraction peaks indicate that the uncalcined products are well crystalline. All diffraction peaks can be perfectly indexed to the anatase phase of TiO_2 (JCPDS 21-1272). No characteristic peaks of other impurities are detected in the XRD pattern, indicating that the F-doped TiO_2 microspheres with high purity could be obtained under current facile synthetic conditions. Calcination at 500°C for 2 h does not change the phase and composition of the hydrangea-like F-doped TiO_2 microspheres.

The morphologies and microstructures of the hydrangea-like F-doped TiO_2 microspheres were characterized by scanning electron microscopy (SEM). Figure 2(a) shows a low-magnification SEM image of the as-prepared sample, which performs that the products consist of large-scale microspheres. The average external diameter of the microspheres is 2.85 μm, as observed by measuring 100 microspheres. A high-magnification SEM image (Figure 2(b)) reveals that the as-prepared products are hydrangea-like with many randomly attached petal-like structures. Moreover, the surface of the petal is not smooth but is composed of numerous TiO_2 nanoparticles (as shown in Figure 2(c)). The morphology and the size of the hydrangea-like TiO_2 microspheres remain unchanged, while it was calcined at 500°C for 2 h (see Figures 2(d)–2(f)). The typical TEM images of the hydrangea-like microspheres before and after calcination at 500°C for 2 h are shown in Figure 3, and it is clear that the microsphere is solid with an external diameter of about 2.87 μm, which is in agreement with the SEM observation.

It has been found that both NH_4F and H_2O_2 play important roles in the formation of the hydrangea-like structures. Without any addition of NH_4F and H_2O_2, no precipitation can be obtained. Increasing H_2O_2 dosage to 15 mg without

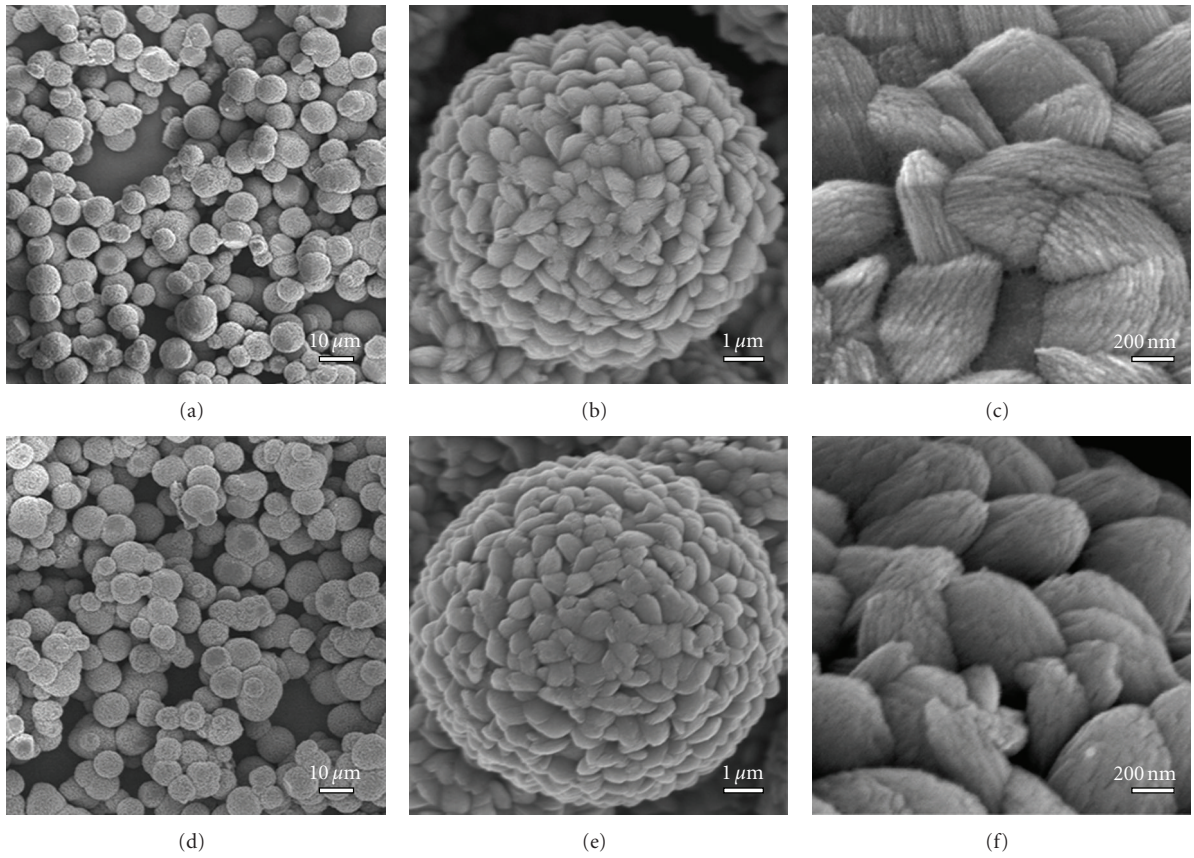

Figure 2: SEM images of the hydrangea-like F-doped TiO_2 microspheres (a, b, c) before and (d, e, f,) after calcinations at 500°C.

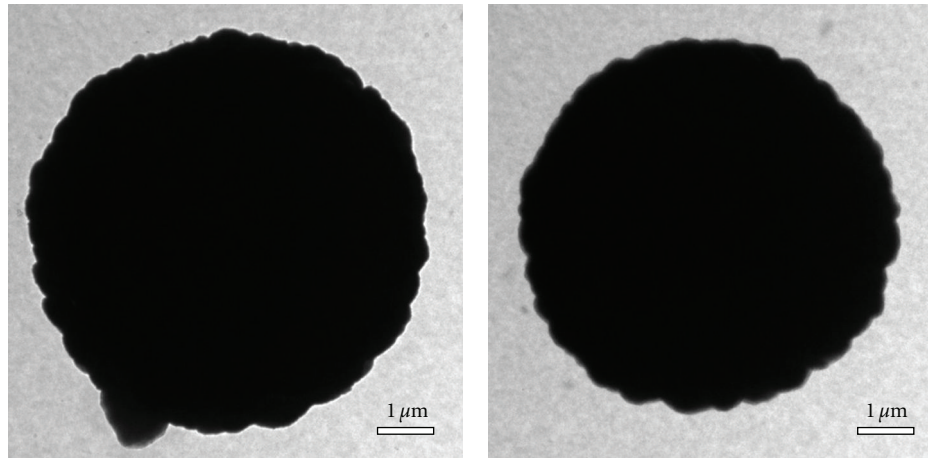

Figure 3: TEM images of the hydrangea-like F-doped TiO_2 microspheres (a) before and (b) after calcinations at 500°C.

adding any NH_4F, only aggregated nanoparticles can be observed. These two experiments indicate that the formation of hydrangea-like microspheres can be attributed to the HF generated during the hydrothermal process [17]. In addition, it has been found that microspheres closely packed with needle-like nanostructures could still be obtained when NH_4F was replaced by NaF, while no microspheres could be produced when NH_4Cl was used. This further confirms the crucial role of HF for the formation of hydrangea-like microspheres (see Figures 4(a) and 4(b)). Furthermore, the

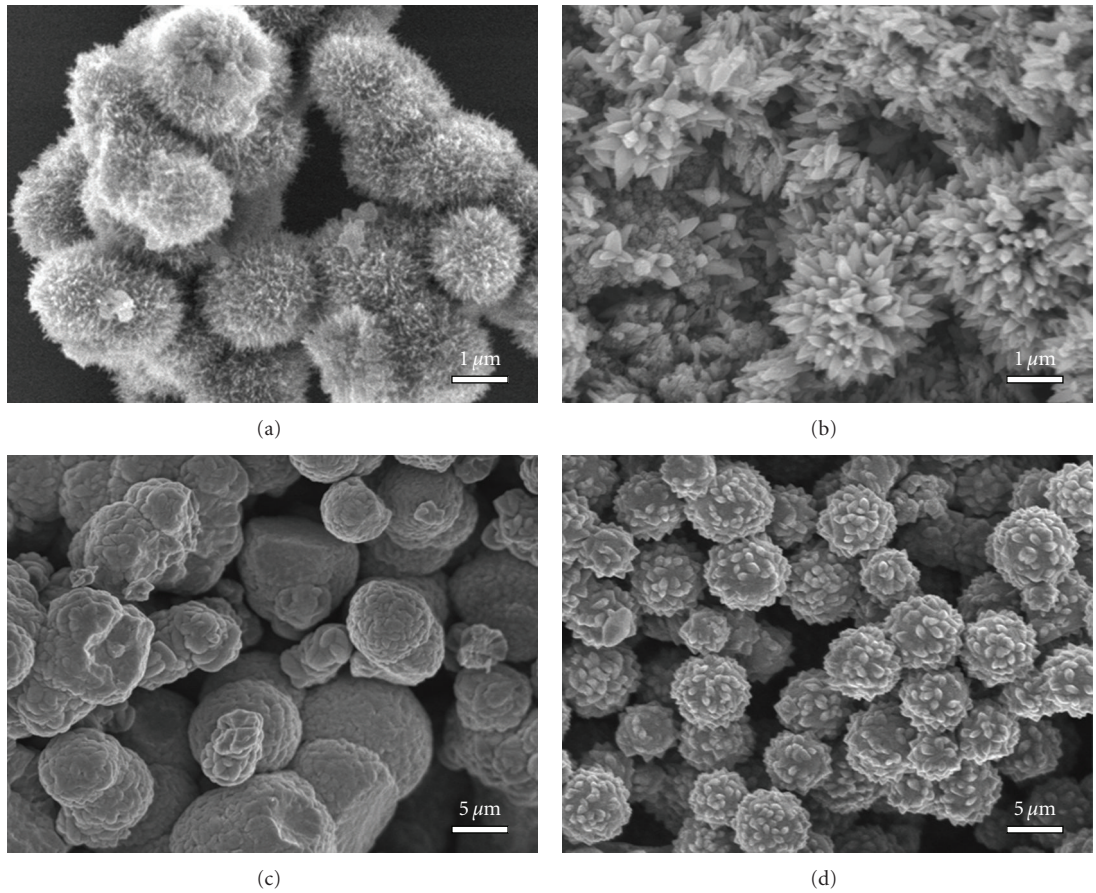

Figure 4: SEM images of the as-prepared samples prepared hydrothermally (a) replaced NH_4F by NaF, (b) replaced NH_4F by NH_4Cl, (c) 10 mL of H_2O_2, and (d) 30 mL of H_2O_2 under the same conditions as those of the hydrangea-like F-doped TiO_2 microspheres.

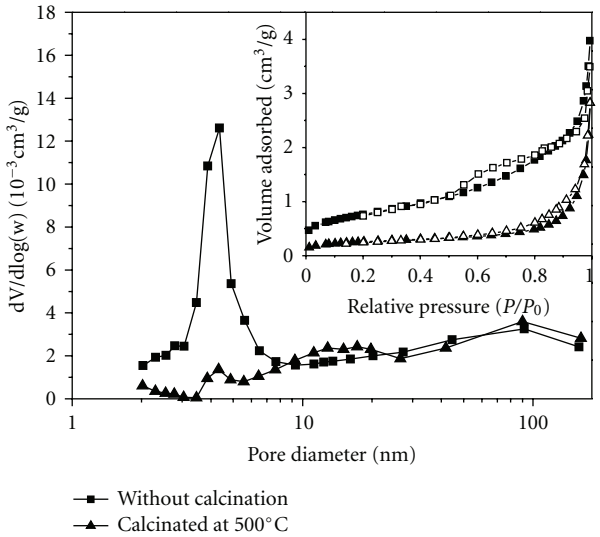

Figure 5: (a) Nitrogen adsorption-desorption isotherm and (b) BJH pore-size distribution curve of the hydrangea-like F-doped TiO_2 microspheres before and after calcinations at 500°C.

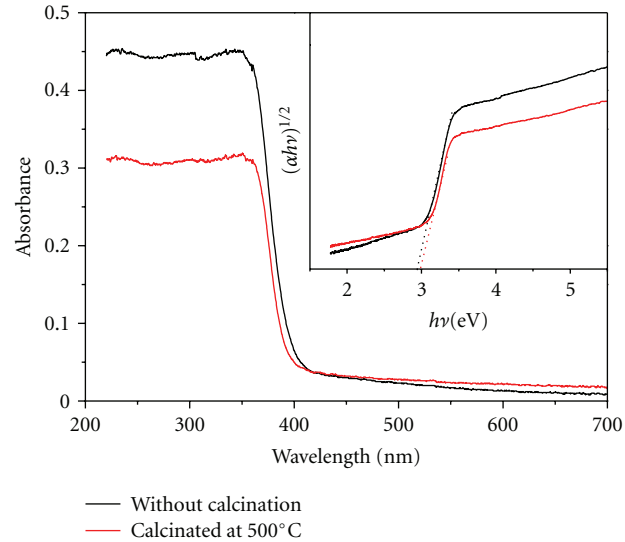

Figure 6: UV-vis absorbance spectra of the hydrangea-like F-doped TiO_2 microspheres before and after calcination. The inset shows the plot of $(\alpha h\nu)^{1/2}$ versus the $(h\nu)$.

hydrangea-like microspheres could only be obtained when suitable amount of H_2O_2 was added in the reaction system (as shown in Figures 4(c) and 4(d)).

Figure 5(a) shows the nitrogen adsorption-desorption isotherms of the hydrangea-like F-doped TiO_2 microspheres before and after calcinations at 500°C. Before calcination, the

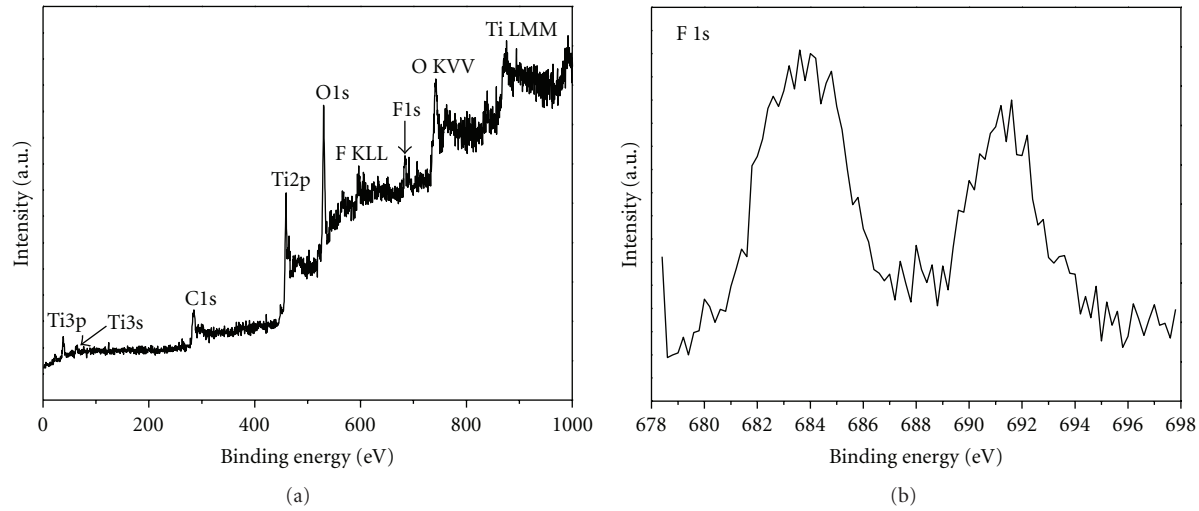

Figure 7: (a) XPS survey spectra and (b) high-resolution XPS spectra of the F 1s region taken on the hydrangea-like F-doped TiO_2 microspheres.

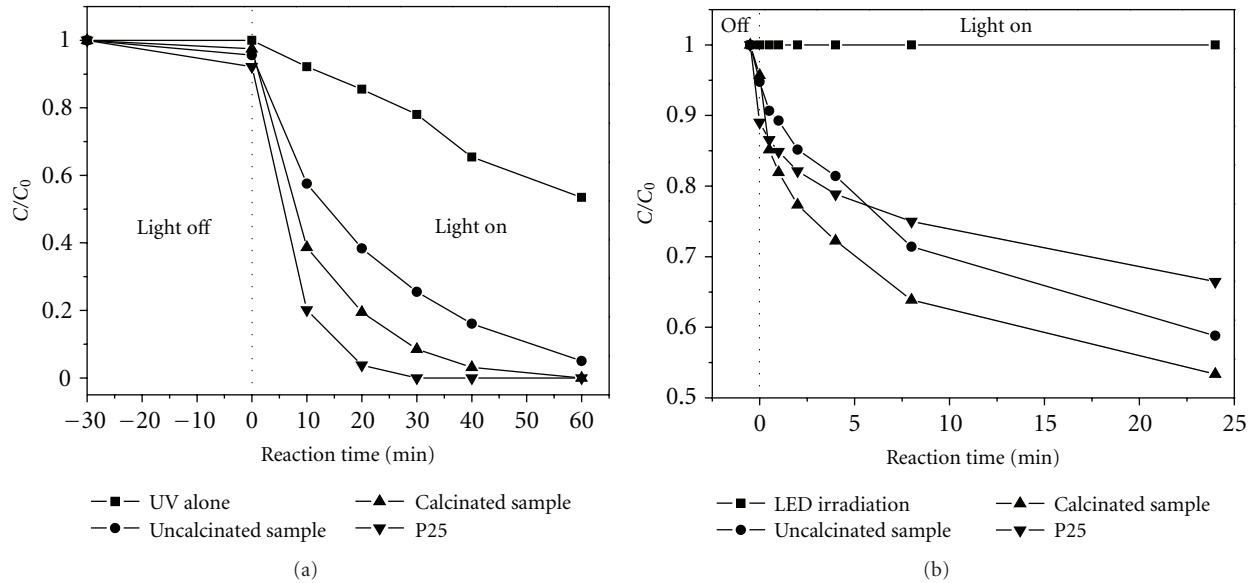

Figure 8: Photodegradation of carbamazepine under (a) UV and (b) blue LED light irradiation.

isotherms are of the typical type IV pattern with distinct H_2 and H_3 hysteretic loops in the range of 0.4–0.9 P/P_0 and 0.9–1.0 P/P_0, respectively, indicating the existence of ink-bottle and slit-shaped pores according to the IUPAC classification [18]. It has been pointed out that the bimodal pores are beneficial to the enhancement of photocatalytic performance due to faster diffusion of various reactants and byproducts [19]. After calcinations at 500°C, the hysteresis loops shifted to a higher relative pressure (P/P_0) range and the area of the hysteresis loops gradually became smaller. This indicates the increase of average pore size and the decrease of pore volume [20]. The corresponding pore size distribution of the hydrangea-like F-doped TiO_2 microspheres (see Figure 5(b)) was determined using the Barrett-Joyner-Halenda (BJH) method from the desorption branch of the isotherm. The BET surface area and average pore diameter of the hydrangea-like F-doped TiO_2 microspheres before and after calcination are 2.74 m^2/g and 8.0 nm, 1.03 m^2/g, and 20.5 nm, respectively.

The optical band gaps of hydrangea-like F-doped TiO_2 microspheres before and after calcination were studied by the UV-vis optical absorbance spectrum. The relationship between the absorption coefficient (α) and the photon energy ($h\nu$) can be written as shown in (1) [21]:

$$(ahv)^n = B\left(E - E_g\right), \tag{1}$$

where B is the constant related to the effective masses associated with the valence and conduction bands, $E = h\nu$ is the

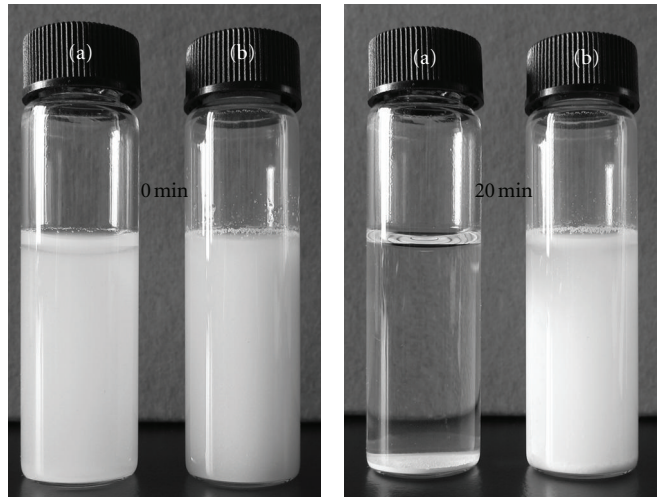

(a) (b)

Figure 9: Sedimentation for 20 min in aqueous suspensions of (a) hydrangea-like titania microspheres and (b) Degussa P25.

photon energy, E_g is the band gap energy, and $n = 1/2$ or 2, depending on whether the transition is indirect or direct. Figure 6 shows the absorption spectra of the hydrangea-like F-doped TiO_2 microspheres before and after calcination. The inset shows the plots of $(\alpha h\nu)^{1/2}$ versus the $(h\nu)$. The band gap energy (E_g) for the samples can be calculated by extrapolating the linear portion of $(\alpha h\nu)^{1/2}$ versus the $(h\nu)$ plot to $\alpha = 0$. On the basis of these results, the optical band gaps for the products before and after calcinations are 2.92 and 2.97, respectively, which are lower than that of Degussa P25 TiO_2 (E_g = 3.18–3.28 eV [22, 23]). The slight redshift of the optical band gap might be the result of F^- anions successfully doped in the hydrangea-like TiO_2 microspheres [8, 24].

X-ray photoelectron spectroscopy (XPS) measurements were carried out to confirm the chemical compositions and the existence forms of the elements in the F-doped TiO_2 microspheres. The results are shown in Figure 7. In the spectrum, elements of Ti, F, O, and C can be observed. The C 1s at 284.6 eV is due to the adventitious hydrocarbon originated from the instrument itself. Figure 7(b) gives the high resolution XPS spectra of F 1s regions from the surfaces of the sample. It can be seen that there are two kinds of F states observed in the F 1s XPS spectrum. The low binding energy of around 683.8 eV could be ascribed to the F^- anions physically adsorbed on the surface of TiO_2, while the high binding energy located at 691.2 eV could be ascribed to the F atoms substituting for the O atoms, forming the Ti-F bonds [8, 25].

Figure 8(a) shows the degradation curves of carbamazepine as a function of reaction time in the presence of different photocatalysts under UV light irradiation. The removal rate dramatically increases with the addition of calcinated F-doped TiO_2 microspheres, which is comparable to that of well-known commercial photocatalyst Degussa P25. The good photocatalytic activity of the products may be caused by the following three factors. First, the physically adsorbed F^- anions on the surface of TiO_2 can increase the photocatalytic degradation efficiency since the ·OH radicals generated on F-TiO_2 surface are more mobile than those generated on pure TiO_2 under UV irradiation [8, 26, 27]. Second, the enhancement of anatase crystallization can accelerate the transmission rate of photogenerated electrons and holes, and thus the photocatalytic activity of TiO_2 is improved [28]. Third, the unique nanostructures are beneficial to the enhancement of photocatalytic performance due to faster diffusion of the reactant and byproducts [14].

The degradation curves of carbamazepine in the presence of hydrangea-like F-doped TiO_2 microspheres before and after calcination under blue LED light (~470 nm) irradiation are shown in Figure 8(b). It has been found that LED light irradiation has no effect on the carbamazepine removal, no more than 0.5% of carbamazepine could be decomposed even after 24 h irradiation. It can also be seen that under identical conditions, the calcinated F-doped TiO_2 microspheres possesses the highest removal efficiency. Though the removal rate of carbamazepine is only 46.7% at the reaction time of 24 h, the use of LED as the light source will make the application of heterogeneous photocatalysis practical since LED is now widely used in daily life.

Microspheres have taken an advantage over powder catalysts for separating the catalyst from solution by filtration or sedimentation. In our experimental, the TiO_2 hollow microspheres can be separated from an aqueous suspension in less than 4 h by sedimentation (as shown in Figure 9), while the aqueous suspension of Degussa P25 is still turbid even after several days.

4. Conclusions

In summary, we report the hydrothermal synthesis of hydrangea-like F-doped TiO_2 microspheres without using any templates or surfactants. It has been found that both of the NH_4F and H_2O_2 dosages have important effects on the

formation of the hydrangea-like structures. The hydrangea-like F-doped TiO_2 microspheres calcined at 500°C exhibits higher photocatalytic activity than that of Degussa P25 under both UV and visible light irradiation. The enhanced photocatalytic activity can be attributed to the successful fluorine doping, good crystallinity, and the unique nanostructures. In addition, the use of LED as the light source will make the application of heterogeneous photocatalysis in practice possible.

Acknowledgments

This work was financially supported by the National Natural Science Foundation of China (Grant no. 51108406) and the Fundamental Research Funds for the Central Universities (2011FZA4022), to the authors we are grateful.

References

[1] A. Markowska-Szczupak, K. Ulfig, and A. W. Morawski, "The application of titanium dioxide for deactivation of bioparticulates: an overview," *Catalysis Today*, vol. 169, no. 1, pp. 249–257, 2011.

[2] M. Ye, Z. Chen, X. Liu, Y. Ben, and J. Shen, "Ozone enhanced activity of aqueous titanium dioxide suspensions for photodegradation of 4-chloronitrobenzene," *Journal of Hazardous Materials*, vol. 167, no. 1–3, pp. 1021–1027, 2009.

[3] Y. P. Guo, S. G. Yang, X. F. Zhou, C. Lin, Y. J. Wang, and W. F. Zhang, "Enhanced photocatalytic activity for degradation of methyl orange over silica-titania," *Journal of Nanomaterials*, vol. 2011, Article ID 296953, 9 pages, 2011.

[4] S. Sakthivel, M. Janczarek, and H. Kisch, "Visible light activity and photoelectrochemical properties of nitrogen-doped TiO_2," *Journal of Physical Chemistry B*, vol. 108, no. 50, pp. 19384–19387, 2004.

[5] S. Livraghi, M. C. Paganini, E. Giamello, A. Selloni, C. Di Valentin, and G. Pacchioni, "Origin of photoactivity of nitrogen-doped titanium dioxide under visible light," *Journal of the American Chemical Society*, vol. 128, no. 49, pp. 15666–15671, 2006.

[6] H. Yang and X. Zhang, "Synthesis, characterization and computational simulation of visible-light irradiated fluorine-doped titanium oxide thin films," *Journal of Materials Chemistry*, vol. 19, no. 37, pp. 6907–6914, 2009.

[7] J. Ryu and W. Choi, "Effects of TiO_2 surface modifications on photocatalytic oxidation of arsenite: the role of superoxides," *Environmental Science and Technology*, vol. 38, no. 10, pp. 2928–2933, 2004.

[8] J. C. Yu, J. Yu, W. Ho, Z. Jiang, and L. Zhang, "Effects of F-doping on the photocatalytic activity and microstructures of nanocrystalline TiO_2 powders," *Chemistry of Materials*, vol. 14, no. 9, pp. 3808–3816, 2002.

[9] Q. Xiang, J. Yu, and M. Jaroniec, "Tunable photocatalytic selectivity of TiO_2 films consisted of flower-like microspheres with exposed 001 facets," *Chemical Communications*, vol. 47, no. 15, pp. 4532–4534, 2011.

[10] S. Liu, J. Yu, and M. Jaroniec, "Anatase TiO_2 with dominant high-energy 001 facets: synthesis, properties, and applications," *Chemistry of Materials*, vol. 23, no. 18, pp. 4085–4093, 2011.

[11] Y. Xie, Y. Li, and X. Zhao, "Low-temperature preparation and visible-light-induced catalytic activity of anatase F-N-codoped TiO_2," *Journal of Molecular Catalysis A*, vol. 277, no. 1-2, pp. 119–126, 2007.

[12] H. Park and W. Choi, "Effects of TiO_2 surface fluorination on photocatalytic reactions and photoelectrochemical behaviors," *Journal of Physical Chemistry B*, vol. 108, no. 13, pp. 4086–4093, 2004.

[13] X. Z. Li, H. Liu, L. F. Cheng, and H. J. Tong, "Photocatalytic oxidation using a new catalyst—TiO_2 microsphere—For water and wastewater treatment," *Environmental Science and Technology*, vol. 37, no. 17, pp. 3989–3994, 2003.

[14] J. Yu, H. Guo, S. A. Davis, and S. Mann, "Fabrication of hollow inorganic microspheres by chemically induced self-transformation," *Advanced Functional Materials*, vol. 16, no. 15, pp. 2035–2041, 2006.

[15] J. H. Pan, X. Zhang, A. J. Du, D. D. Sun, and J. O. Leckie, "Self-etching reconstruction of hierarchically mesoporous F-TiO_2 hollow microspherical photocatalyst for concurrent membrane water purifications," *Journal of the American Chemical Society*, vol. 130, no. 34, pp. 11256–11257, 2008.

[16] M. M. Ye, Q. Zhang, Y. X. Hu et al., "Magnetically recoverable core-shell nanocomposites with enhanced photocatalytic activity," *Chemistry*, vol. 16, no. 21, pp. 6243–6250, 2010.

[17] M. Ye, Y. Yang, T. Zhang, Y. Shao, and C. Li, "Template-free hydrothermal synthesis of macroporous TiO_2 microspheres on a large scale," *Materials Letters*, vol. 65, no. 15-16, pp. 2384–2387, 2011.

[18] K. S. W. Sing, D. H. Everett, R. A. W. Haul et al., "Reporting physisorption data for gas solid systems with special reference to the determination of surface-area and porosity," *Pure and Applied Chemistry*, vol. 57, no. 4, pp. 603–619, 1985.

[19] Y. Chen and D. D. Dionysiou, "Bimodal mesoporous TiO_2-P25 composite thick films with high photocatalytic activity and improved structural integrity," *Applied Catalysis B*, vol. 80, no. 1-2, pp. 147–155, 2008.

[20] J. Yu, M. Zhou, B. Cheng, and X. Zhao, "Preparation, characterization and photocatalytic activity of in situ N,S-codoped TiO_2 powders," *Journal of Molecular Catalysis A*, vol. 246, no. 1-2, pp. 176–184, 2006.

[21] N. Serpone, D. Lawless, and R. Khairutdinov, "Size effects on the photophysical properties of colloidal anatase TiO_2 particles: size quantization or direct transitions in this indirect semiconductor?" *Journal of Physical Chemistry*, vol. 99, no. 45, pp. 16646–16654, 1995.

[22] M. Ye, Z. Chen, W. Wang, J. Shen, and J. Ma, "Hydrothermal synthesis of TiO_2 hollow microspheres for the photocatalytic degradation of 4-chloronitrobenzene," *Journal of Hazardous Materials*, vol. 184, no. 1–3, pp. 612–619, 2010.

[23] Z. Liu, D. D. Sun, P. Guo, and J. O. Leckie, "One-step fabrication and high photocatalytic activity of porous TiO_2 hollow aggregates by using a low-temperature hydrothermal method without templates," *Chemistry*, vol. 13, no. 6, pp. 1851–1855, 2007.

[24] G. Yang, Z. Jiang, H. Shi et al., "Study on the photocatalysis of F-S co-doped TiO_2 prepared using solvothermal method," *Applied Catalysis B*, vol. 96, no. 3-4, pp. 458–465, 2010.

[25] Y. huo, Y. jin, J. zhu, and H. li, "Highly active $TiO_{2-x-y}N_xF_y$ visible photocatalyst prepared under supercritical conditions in NH_4F/EtOH fluid," *Applied Catalysis B*, vol. 89, no. 3-4, pp. 543–550, 2009.

[26] J. Yu, W. Wang, B. Cheng, and B. L. Su, "Enhancement of photocatalytic activity of Mesporous TiO_2 powders by hydrothermal surface fluorination treatment," *Journal of Physical Chemistry C*, vol. 113, no. 16, pp. 6743–6750, 2009.

[27] S. Liu, J. Yu, and M. Jaroniec, "Tunable photocatalytic selectivity of hollow TiO_2 microspheres composed of anatase polyhedra with exposed 001 facets," *Journal of the American Chemical Society*, vol. 132, no. 34, pp. 11914–11916, 2010.

[28] J. Yu, L. Zhang, B. Cheng, and Y. Su, "Hydrothermal preparation and photocatalytic activity of hierarchically sponge-like macro-/mesoporous Titania," *Journal of Physical Chemistry C*, vol. 111, no. 28, pp. 10582–10589, 2007.